DOI: 10.1002/ejic.200801170

Self-Assembly from Discrete Clusters to 2D Network Based on $[Fe(phen)(CN)_4]^-$ and $[Fe(bipy)(CN)_4]^-$: Synthesis, Structures and Magnetic Properties

Hua Xiang,[a] Shao-Jun Wang,[a] Long Jiang,[a] Xiao-Long Feng,[a] and Tong-Bu Lu*[a]

Keywords: Iron / Nickel / Macrocyclic ligands / Bridging ligands / Magnetic properties

A series of cyanido-bridged complexes $\{[Fe^{III}(phen)(CN)_4]_2[NiL^1]\}\cdot 4H_2O$ (**1**), $\{[Fe^{III}(bipy)(CN)_4]_2[NiL^1]\}\cdot 4H_2O$ (**2**), $[Fe^{III}(bipy)(CN)_4]_2[NiL^2]$ (**3**), $\{[Fe^{III}(phen)(CN)_4]_2[CuL^3]\}\cdot 5H_2O$ (**4**), $\{[Fe^{II}(phen)(CN)_4][Ni(ea)_2]\}_2\cdot 2H_2O$ (**5**), $\{[Fe^{II}(phen)(CN)_4][NiL^2]\cdot 2H_2O\}_n$ (**6**), $\{[Fe^{III}(bipy)(CN)_4]_2[Ni(H_2O)_2]\}\cdot 6.5H_2O\}_n$ (**7**) and $\{[Fe^{II}(bipy)(CN)_4][Ni(ea)_2]\cdot H_2O\}_n$ (**8**) were synthesized using $H[Fe(phen)(CN)_4]\cdot 2H_2O$ and $H[Fe(bipy)(CN)_4]\cdot 2H_2O$ as precursors [L^1 = 5,5,7,12,12,14-hexamethyl-1,4,8,11-tetraazacyclotetradecane, L^2 = 3,10-bis(2-phenylethyl)-1,3,5,8, 10,12-hexaazacyclotetradecane, L^3 = 3,10-bis(2-hydroxyethyl)-1,3,5,8,10,12-hexaazacyclotetradecane, phen = 1,10-phenanthroline, bipy = 2,2′-bipyridine, ea = ethanolamine). Complexes **1**–**4** are trinuclear clusters, and **5** is a tetranuclear square. In **6**, the $[Fe^{II}(phen)(CN)_4]^{2-}$ anions alternately bridge the $[NiL^2]^{2+}$ cations to generate a 1D wavy chain. The structure of **7** possesses a 4,2-ribbonlike chain, which contains a $Ni^{II}_2(CN)_4Fe^{III}_2$ square with each Ni^{II} atom shared by two adjacent squares. Each Fe^{II} and Ni^{II} atom in **8** acts as a three-connected node through the cyanido-bridges to generate a 2D network with a $4,8^2$ topological net. Ferromagnetic couplings are found between the low-spin Fe^{III} ions and the Ni^{II} ions through the cyanido groups in **1**–**3** and **7**, and a metamagnetic behavior and a frequency dependence of the out-of-phase ac susceptibility are observed in **7**.

Introduction

Over the past two decades, research in the area of the self-assembly of cyanido-bridged metal complexes has been active,[1] which has resulted in a great number of cyanido-bridged metal complexes. These complexes show a wide range of useful properties and can be used as hydrogen adsorption and storage materials,[2] catalysts,[3] molecular sieves,[4] room temperature magnets,[5] electrochemically tunable magnets,[6] chiral magnets,[7] single-molecule magnets (SMMs),[8] single-chain magnets (SCMs)[9] and metamagnets,[10] and spin-crossover[11] and charge-transfer complexes.[12] One of the main synthesis routes of such complexes is to react preformed $[B(L_B)(CN)_y]^{(y+l-b)-}$ anions with fully solvated $[A(H_2O)_6]^{a+}$ cations or partially coordinated $[A(L_A)(H_2O)_x]^{(a-l)+}$ cations (A/B = transition-metal ions, L_A/L_B = polydentate ligand, l = charge of L_A/L_B, a = charge of A, and b = charge of B).[11d,13] The precursors of $[M(phen)(CN)_4]^-$ and $[M(bipy)(CN)_4]^-$ are involved in self-assembly to form various cyanido-bridged dimetallic complexes from discrete clusters to 3D frameworks[9a,9b,13–24] (M = Fe^{III}, Cr^{III}; phen = 1,10-phenanthroline; bipy = 2,2′-bipyridine), and some of these complexes show interesting magnetic properties. SCM behavior was observed in 4,2-ribbonlike chains of $\{[Fe^{III}(phen)(CN)_4]_2[Co^{II}(H_2O)_2]\}\cdot 4H_2O$ and $\{[Fe^{III}(bipy)(CN)_4]_2[Co^{II}(H_2O)_2]\}\cdot 4H_2O$,[9a] spin-canting and metamagnetic behavior were observed in a double zigzag chain of $\{[Cr^{III}(bipy)(CN)_4]_2[Mn^{II}(H_2O)]\}\cdot H_2O\cdot CH_3CN$,[15] metamagnetic behavior was found in a 2D network of $\{[Cr^{III}(phen)(CN)_4]_2[Mn^{III}(N_3)(CH_3OH)]\}\cdot CH_3OH$,[19] and spin-flopping behavior was observed in a 2D network of $\{[Cr^{III}(phen)(CN)_4](Mn^{II}(\mu\text{-ox})_{0.5}(H_2O))\}$ (ox = oxalate).[24]

To expand the rich magnetic properties and to better understand the magneto–structural relationship of cyanido-bridged dimetallic assemblies based on such precursors, $[Fe(phen)(CN)_4]^-$ and $[Fe(bipy)(CN)_4]^-$ were treated with macrocyclic complexes $[ML]^{2+}$ and $[Ni(ea)_2(H_2O)_2]^{2+}$ to synthesize a series of dimetallic assemblies from discrete clusters to 2D networks [M = Ni^{II}, Cu^{II}; L = 5,5,7,12,12,14-hexamethyl-1,4,8,11-tetraazacyclotetradecane (L^1), 3,10-bis(2-phenylethyl)-1,3,5,8,10,12-hexaazacyclotetradecane (L^2), and 3,10-bis(2-hydroxyethyl)-1,3,5,8,10,12-hexaazacyclotetradecane (L^3), see Scheme 1]. Their synthesis, structures, and magnetic properties are presented in this paper.

[a] MOE Key Laboratory of Bioinorganic and Synthetic Chemistry / State Key Laboratory of Optoelectronic Materials and Technologies / School of Chemistry and Chemical Engineering, Sun Yat-Sen University,
Guangzhou 510275, China
Fax: +86-20-84112921
E-mail: lutongbu@mail.sysu.edu.cn
Supporting information for this article is available on the WWW under http://www.eurjic.org or from the author.

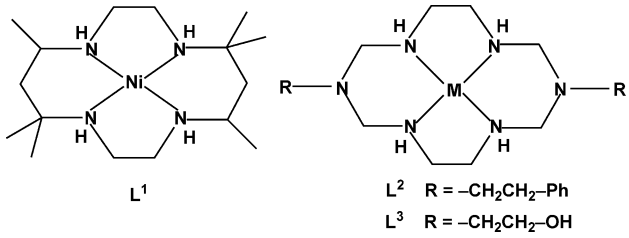

Scheme 1. The structures of L^1, L^2, and L^3.

Results and Discussion

Preparation Chemistry

The layering of an aqueous solution of H[Fe(phen)-$(CN)_4$]·$2H_2O$ or H[Fe(bipy)$(CN)_4$]·$2H_2O$ with an acetonitrile solution of the macrocyclic complexes $[ML](ClO_4)_2$ generated four cyanido-bridged trinuclear clusters $\{[Fe^{III}(phen)(CN)_4]_2[NiL^1]\}$·$4H_2O$ (**1**), $\{[Fe^{III}(bipy)(CN)_4]_2$-$[NiL^1]\}$·$4H_2O$ (**2**), $[Fe^{III}(bipy)(CN)_4]_2[NiL^2]$ (**3**), and $\{[Fe^{III}(phen)(CN)_4]_2[CuL^3]\}$·$5H_2O$ (**4**). The layering of an aqueous solution of H[Fe(phen)$(CN)_4$]·$2H_2O$ with an acetonitrile solution of $[NiL^2](ClO_4)_2$ gave the 1D chain $\{[Fe^{II}(phen)(CN)_4][NiL^2]$·$2H_2O\}_n$ (**6**); Fe^{III} is reduced to Fe^{II} during the reaction, which is a common phenomenon in cyanidoiron(III) compounds.[25] This phenomenon was also observed in the preparation of the neutral tetranuclear cluster $\{[Fe^{II}(phen)(CN)_4][Ni(ea)]\}_2$·$2H_2O$ (**5**) and the 2D network of $\{[Fe^{II}(bipy)(CN)_4][Ni(ea)_2]$·$H_2O\}_n$ (**8**), which were obtained by layering a mixture of $Ni(ClO_4)_2$·$6H_2O$ and ethanolamine (ea) in acetonitrile with an aqueous solution of H[Fe(phen)$(CN)_4$]·$2H_2O$ or H[Fe(bipy)$(CN)_4$]·$2H_2O$. A similar reaction of $Ni(ClO_4)_2$·$6H_2O$ with H[Fe(bipy)$(CN)_4$]·$2H_2O$ in the presence of malonic acid led to the formation of a 1D 4,2-ribbonlike chain, $\{[Fe^{III}(bipy)(CN)_4]_2[Ni(H_2O)_2]$·$6.5H_2O\}_n$ (**7**). In the IR spectra of **1**–**8**, the occurrence of two peaks corresponding to CN stretching vibrations demonstrates the presence of bridging and terminal cyanido groups (Scheme 2).

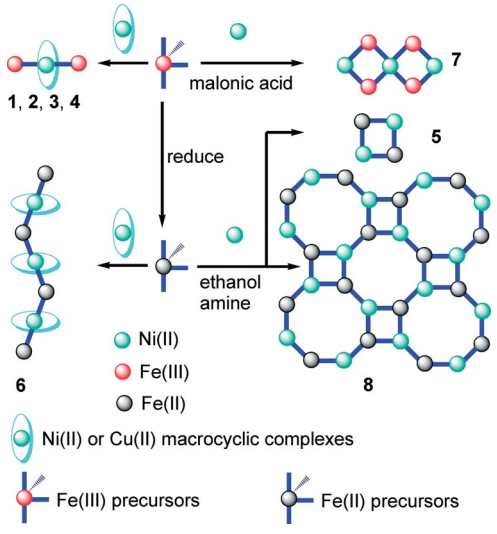

Scheme 2. Self-assembly based on H[Fe(phen)$(CN)_4$]·$2H_2O$ and H[Fe(bipy)$(CN)_4$]·$2H_2O$.

Crystal Structures

Discrete Clusters of 1–5

Complexes **1**–**4** have similar structures that consist of centrosymmetric trinuclear entities. The crystallographic data are presented in Table 1. The structure of **1** is illustrated in Figure 1, while those of **2**–**4** are shown in Figure S1. Each Fe^{III} atom in **1**–**4** is coordinated by two nitrogen atoms from the phen/bipy group and four carbon atoms from four cyanido groups, which leads to a distorted octahedral FeN_2C_4 geometry. The Fe–N distances are longer than the Fe–C distances. Each Ni^{II}/Cu^{II} atom lies on an inversion center and is coordinated to four secondary nitrogen atoms from the macrocyclic ligands at the equatorial positions and two nitrogen atoms from two individual cyanido groups of $[Fe(phen)(CN)_4]^-$ or $[Fe(bipy)(CN)_4]^-$ in the axial positions to form a distorted MN_6 octahedral geometry. The six Ni–N bond lengths of **1**–**3** are similar and vary over a narrow range from 2.018(1) Å to 2.111(3) Å, while the axial Cu–N_{CN} distances [2.530(9) Å] are much longer than the equatorial Cu–N distances [1.992(9)–1.994(8) Å] because of the Jahn–Teller effect of an octahedral Cu^{II} ion. The values of the terminal Fe–C≡N angles [174.8(11)–178.7(4)°] are close to those of the bridging Fe–C≡N angles [174.8(3)–

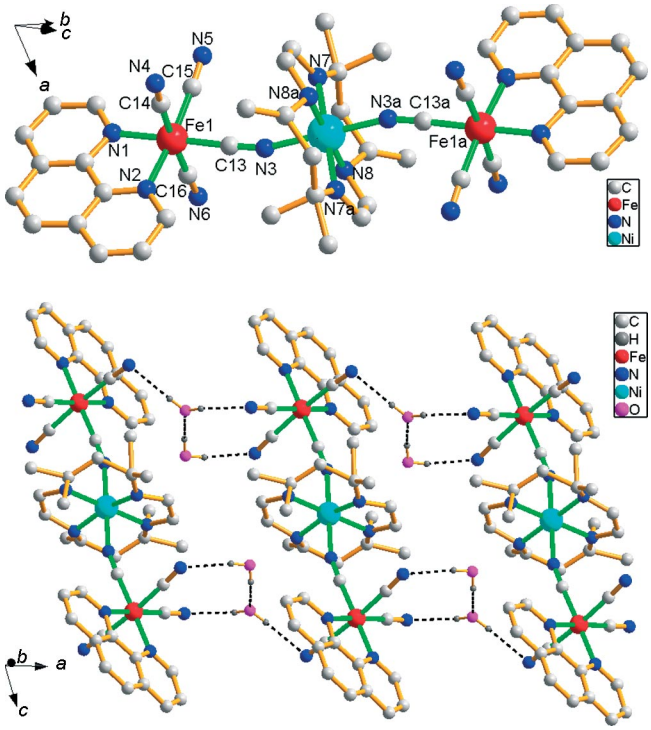

Figure 1. The structure of **1** (top) and the fragment of 1D hydrogen-bonded ladderlike chain (bottom). Symmetry code a: $-x, -y + 1, -z + 1$.

177.6(2)°]. While the Ni–N≡C angles in **1**–**3** deviate significantly from 180° [163.5(3)° in **1**; 163.69(2)° in **2**; 165.7(3)° in **3**], the Cu–N≡C angle [137.2(9)°] in **4** is much smaller than the Ni–N≡C angles in **1**–**3**, which results in similar values for the intramolecular Fe···Cu distance (5.128 Å) in **4** and for the intramolecular Fe···Ni distances (5.082–5.107 Å) in **1**–**3**, although there is significant elongation of the Cu–N_{CN} distances. The trinuclear units in **1** and **2** are linked through intermolecular hydrogen-bonding interactions between the water molecules and the terminal cyanido groups (see Table S2 and Figure 1) to form a 1D ladderlike chain, and the 1D ladderlike chains are further connected through intermolecular π···π interactions between two adjacent phen/bipy groups to generate a 2D sheet (Figure S2a). The shortest centroid··· centroid distance is 3.618 Å in **1** and 3.833 Å in **2**. The trinuclear units in **3** are linked through edge-to-face C–H···π interactions between two adjacent bipy molecules to form a 1D chain (Figure S2b), with a C(9)–H(9)···centroid angle of 70.6° and a H(9)···centroid separation of 2.702 Å. In **4**, the trinuclear units are linked through intermolecular hydrogen-bonding interactions between the terminal cyanido groups and the nitrogen atoms of L^3 to form a 1D ladderlike chain (Figure S2c). The 1D chains are further held together through intermolecular hydrogen-bonding interactions between the water molecules, the hydroxy groups of L^3, and the terminal cyanido groups to form a 3D structure (Figures S2d).

The structure of **5** is different from those of **1**–**4**, in which two $[Fe^{II}(phen)(CN)_4]^{2-}$ anions bridge two $[Ni(ea)_2]^{2+}$ cations through cyanido groups to form [2+2]-type discrete molecular squares (Figure 2). The remaining four coordinated sites of each Ni^{II} are occupied by two ea molecules. The Fe–C distances [1.898(6)–1.935(6) Å] and the Fe–N_{phen} distances [2.000(4) and 2.005(4) Å] are close to those found in **1**–**4** and other reported tetranulcear squares.[17,18,25] The Ni–N_{CN} distances [2.034(5) and 2.054(5) Å] are slightly shorter than those in **1**–**3** [2.095(4)–2.111(3) Å]. Four Fe–

Table 1. Crystallographic data of **1**–**8**.

Compound	**1**	**2**	**3**	**4**
Formula	$C_{48}H_{60}Fe_2N_{16}NiO_4$	$C_{44}H_{60}Fe_2N_{16}NiO_4$	$C_{50}H_{50}Fe_2N_{18}Ni$	$C_{44}H_{56}CuFe_2N_{18}O_7$
F_w	1095.53	1047.49	1073.49	1124.31
Temperature [K]	173(2)	173(2)	173(2)	173(2)
Crystal system	triclinic	triclinic	monoclinic	triclinic
Space group	$P\bar{1}$	$P\bar{1}$	$P2_1/c$	$P\bar{1}$
a [Å]	9.3568(19)	9.2525(14)	10.353(3)	10.0645(15)
b [Å]	10.153(2)	10.2886(16)	13.336(3)	11.072(2)
c [Å]	14.730(3)	14.083(2)	18.104(4)	12.195(4)
α [°]	86.203(4)	80.229(2)	90	68.072(9)
β [°]	71.968(3)	74.079(2)	105.732(4)	88.480(8)
γ [°]	71.311(3)	69.447(2)	90	83.306(8)
V [Å^3]	1259.5(5)	1203.1	2405.8(10)	1251.9(5)
Z	1	1	2	1
D_c [g cm^{-3}]	1.444	1.446	1.482	1.491
μ [mm]$^{-1}$	0.999	1.042	1.040	1.061
θ range [°]	1.45–27.16	1.51–27.06	1.92–27.12	1.80–25.00
Data collected	10575	10109	14252	5066
Unique reflections (R_{int})	5368(0.0250)	5141(0.0209)	5301(0.0747)	4406(0.0803)
R_1, wR_2 [$I > 2\sigma(I)$]	0.0513, 0.1285	0.0350, 0.1007	0.0510, 0.1001	0.0908, 0.2042
R_1, wR_2 (all data)	0.0797, 0.1482	0.0454, 0.1075	0.1066, 0.1184	0.1009, 0.2542
Compound	**5**	**6**	**7**	**8**
Formula	$C_{40}H_{60}Fe_2N_{16}Ni_2O_8$	$C_{38}H_{48}FeN_{12}NiO_2$	$C_{28}H_{33}Fe_2N_{12}NiO_{8.5}$	$C_{18}H_{24}FeN_8NiO_3$
F_w	1122.16	819.44	844.07	515.01
Temperature [K]	173(2)	173(2)	173(2)	173(2)
Crystal system	triclinic	monoclinic	orthorhombic	monoclinic
Space group	$P\bar{1}$	$C2/c$	$Cmcm$	$P2_1/c$
a [Å]	7.313(3)	23.605(4)	24.655(7)	11.857(4)
b [Å]	11.782(4)	10.848(2)	13.615(4)	13.886(5)
c [Å]	14.301(5)	18.503(3)	11.983(4)	13.460(9)
α [°]	103.634(6)	90	90	90
β [°]	99.260(6)	128.556(3)	90	106.288(6)
γ [°]	90.443(6)	90	90	90
V [Å^3]	1180.5(7)	3705.1(12)	4022(2)	2127.21(18)
Z	1	4	4	4
D_c [g cm^{-3}]	1.578	1.469	1.394	1.608
μ [mm]$^{-1}$	1.456	0.953	1.234	1.605
θ range [°]	2.03–26.00	2.18–27.04	1.71–25.00	2.15–25.00
Data collected	8980	9083	8744	9281
Unique reflections (R_{int})	4454(0.0418)	3982(0.0351)	1883(0.0869)	3608(0.1344)
R_1, wR_2 [$I > 2\sigma(I)$]	0.0530, 0.1180	0.0421, 0.1022	0.0748, 0.1953	0.1131, 0.2363
R_1, wR_2 (all data)	0.0993, 0.1408	0.0693, 0.1233	0.1196, 0.2341	0.1441, 0.2590

C≡N angles deviate slightly from 180° [173.9(5) and 178.0(5)°], while two Ni–N≡C angles [154.1(4)°] are more bent than the other two Ni–N≡C angles [175.9(5)°]. The intramolecular Fe···Ni distances of 4.932 and 5.080 Å are close to those previously reported squares.[25] The tetranuclear clusters are further connected through intermolecular hydrogen-bonding interactions between the hydroxy groups of ea and the terminal cyanido groups (Figure S2e).

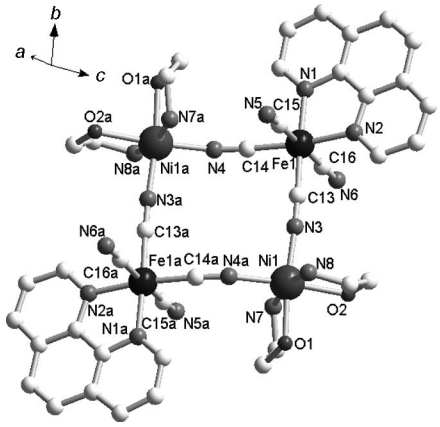

Figure 2. The structure of **5**. Symmetry code a: $-x + 1, -y, -z$.

1D Chain Structures of 6 and 7

The structure of **6** is a 1D wavy chain constructed by alternating $[Fe^{II}(phen)(CN)_4]^{2-}$ anions and $[NiL^2]^{2+}$ cations that are bridged through cyanido groups (Figure 3). The Fe–C distances vary within a small range [1.906(3)–1.924(3) Å], and the Fe–N_{phen} distance [1.988(2) Å] is slightly shorter than those found in **1**–**5**. The values of Ni–N_{CN} [2.054(2) and 2.067(2) Å] are similar to those found in **1**–**5**. It is interesting to note that the Ni–C≡N angle is only 149.5(2)°, which is smaller than those found in **1**–**5**, and leads to the shorter intrachain Fe···Ni distance (4.991 Å). Two water molecules are hydrogen bonded with the nitrogen atoms of two terminal cyanido groups, with an O···N distance of 2.805 Å.

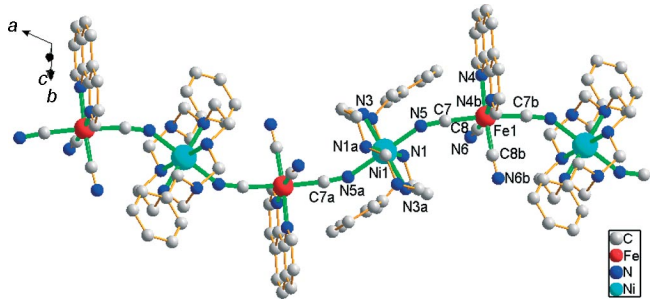

Figure 3. A fragment of the 1D wavy chain in **6**. Symmetry codes a: $-x + 3/2, -y + 3/2, -z + 1$; b: $-x + 1, y, -z + 1/2$.

Compound **7** has a 4,2-ribbonlike chain structure and contains a $Ni^{II}_2(CN)_4Fe^{III}_2$ square with each Ni^{II} atom shared by two adjacent squares (Figure 4). Each Ni^{II} atom in the chain is coordinated to four cyanido nitrogen atoms from four $[Fe^{III}(bipy)(CN)_4]^-$ units in the equatorial plane and to two water molecules in the axial positions. Though the framework of the 4,2-ribbonlike chain of **7** is similar to that of the reported compound $\{[Fe^{III}(bipy)(CN)_4]_2[Ni(H_2O)_2]\}\cdot 4H_2O$ (**9**),[26] there are three main differences between these two compounds. Firstly, the two terminal cyanido groups in **7** are in a *trans* position, while those in **9** are in a *cis* position. Secondly, the Fe^{III} ions and Ni^{II} ions within the chain in **7** are not located in the same plane, which leads to a chain with an X shape along the *c* axis, while those in **9** are almost in the same plane (Figure S3). Thirdly, all the chains in **7** are packed in the same orientation (Figure S3b), while the chains in **9** are packed in two different orientations with an angle of 60.19°. Thus **7** and **9** can be regarded as supramolecular isomers. The different arrangements of **7** and **9** lead to the more bent Ni–N≡C angles in **7** [162.0(6)° in **7**, 167.1(2)° and 171.2(2)° in **9**]. It is very interesting to note that compound **7** can only be obtained in the presence of malonic acid, though malonate anions do not exist within the structure of **7**. Without malonic acid, only **9** is formed.

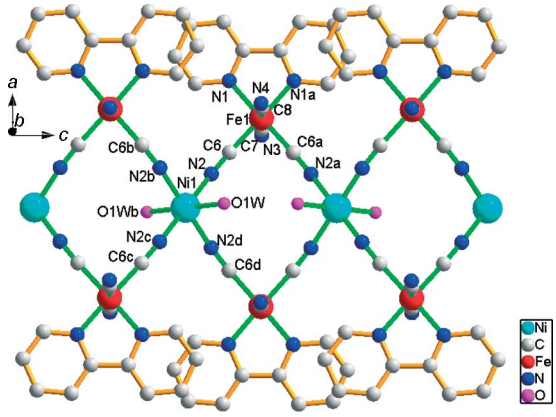

Figure 4. A fragment of the 1D 4, 2-ribbonlike chain in **7**. Symmetry codes a: $x, y, -z + 1/2$; b: $x, -y + 1, -z$; c: $-x, -y + 1, -z$; d: $-x, y, z$.

2D Network of 8

Complex **8** has a cyanido-bridged 2D network structure (Figure 5). Each iron(II) ion is surrounded by a bidentate bipy ligand and four cyanido groups in a distorted FeN_2C_4 environment. The six-coordinate Ni^{II} ion also displays a distorted octahedral geometry by coordinating to three N atoms of the cyanido groups, a bidentate chelating ea molecule, and an oxygen atom from another monodentate ea molecule. Each Fe^{II} and Ni^{II} atoms act as a three-connected node through the cyanido-bridges to generate a 2D network with a $4,8^2$ topological net (Figure 5). The stable 2D networks are further connected by weak π···π interactions of adjacent bipy molecules to generate a 3D supramolecular structure, and the centroid···centroid distance between the two adjacent bipy molecules is 3.605 Å.

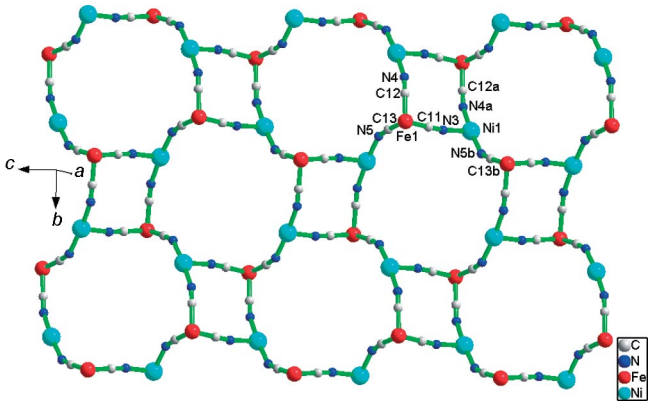

Figure 5. View of a fragment of the 2D network of **8** (water and ea molecules and terminal cyanide groups are omitted for clarity). Symmetry codes a: $-x + 2$, $-y$, $-z + 1$; b: x, $-y + 1/2$, $z - 1/2$.

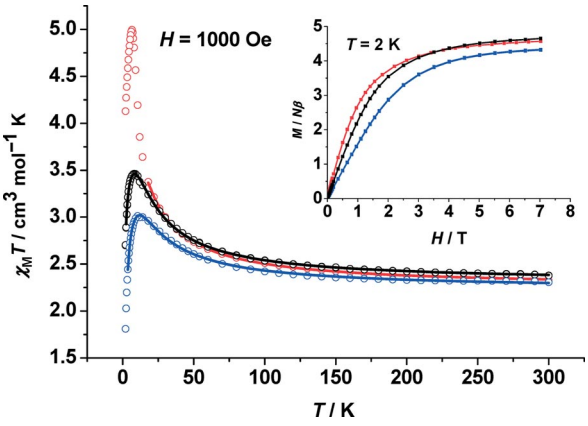

Figure 6. $\chi_M T$ vs. T plots for **1** (black), **2** (red) and **3** (blue) under an applied field of 1000 Oe: (○) experimental data; (solid line) best-fit curve. The inset shows a M vs. H plot at 2.0 K for **1** (black), **2** (red) and **3** (blue).

Magnetic Properties

The magnetic properties of **1**–**3** are similar because of their similar structures. The $\chi_M T$ vs. T plots of **1**–**3** (χ_M is the molar magnetic susceptibility per $Fe^{III}_2Ni^{II}$ unit) are shown in Figure 6. At room temperature, the $\chi_M T$ values are 2.43 (4.41 μ_B), 2.32 (4.27 μ_B), and 2.31 $cm^3 mol^{-1} K$ (4.30 μ_B) for **1**–**3**, respectively. All three values are larger than 1.75 $cm^3 mol^{-1} K$ (3.74 μ_B) expected for the spin-only case from the octahedral Ni^{II} ion ($S_{Ni} = 1$) and two low-spin Fe^{III} centers ($S_{Fe} = 1/2$), which is indicative of an important orbital contribution in **1**–**3**. Upon cooling, the $\chi_M T$ values increase slowly above 50 K, then increase quickly to maximum values of 3.46 $cm^3 mol^{-1} K$ at 8.0 K for **1**, 5.00 $cm^3 mol^{-1} K$ at 6.5 K for **2**, and 3.01 $cm^3 mol^{-1} K$ at 10.5 K for **3**, respectively; below these temperatures, $\chi_M T$ values decrease sharply to a minimum value of 2.70, 4.12, and 1.81 $cm^3 mol^{-1} K$ at 2 K for **1**–**3**, respectively. In addition, the plots of $1/\chi_M$ vs. T in the temperature range 30–300 K obey the Curie–Weiss law with a positive Weiss constant of 7.88(8) K for **1**, 8.65(4) K for **2**, and 6.38(1) K for **3**. These observations clearly suggest that the Ni^{II} and Fe^{III} atoms within the clusters of **1**–**3** are ferromagnetically coupled through the cyanido bridges, as a result of the orthogonality of the t_{2g} magnetic orbitals of Fe^{III} and the e_g magnetic orbitals of Ni^{II}. The M vs. H plots at 2.0 K for **1**–**3** (inset of Figure 6) confirm the ferromagnetic nature of the magnetic coupling. The magnetizations increase quickly at low fields and reach values of 4.64 $N\beta$ for **1**, 4.56 $N\beta$ for **2**, and 4.31 $N\beta$ for **3** at 7 T, which are close to the expected value of 4 $N\beta$. As the trinuclear clusters in **1**–**3** are well separated (the shortest intermolecular Fe···Fe distances are 6.566 Å, 6.577 Å, and 7.909 Å for **1**–**3**, respectively), there is no long-range magnetic order in **1**–**3**, which is supported by the ac susceptibility measurements (Figure S4).

In order to explore the intensities of the ferromagnetic couplings in **1**–**3**, we analyzed the magnetic data through the following Hamiltonian:[27a,27b]

$$\hat{H} = -2JS_{Ni^{II}}(S_{Fe^{III}} + S_{Fe^{III}})$$

$$\chi' = \frac{2N\beta^2 g^2}{kT}\frac{1 + e^{2J/kT} + 5e^{4J/kT}}{3 + e^{-2J/kT} + 3e^{2J/kT} + 5e^{4J/kT}} \qquad \chi = \frac{\chi'}{1 - 2zJ'\chi'/N\beta^2 g^2}$$

where J and J' represent the intramolecular and intermolecular magnetic coupling constants, respectively. The least-squares fit of the magnetic susceptibility data of **1**–**3** gives the fitted values illustrated in Table 2. The value of J in **3** is slightly smaller than those in **1** and **2**, because of slightly longer intramolecular Fe···Ni distance (5.082 Å in **1**, 5.088 Å in **2**, 5.107 Å in **3**) arising from the large volume of the pendant groups of L^2 in **3**.

Table 2. Fitted values for **1**–**3**.

	g	J [cm^{-1}]	zJ' [cm^{-1}]	R[a]
1	2.295(1)	6.85(3)	–0.146(1)	9.7×10^{-6}
2	2.269(1)	6.8(1)	0.08(1)	6.8×10^{-6}
3	2.257(1)	6.62(6)	–0.353(2)	1.0×10^{-5}

[a] $R = \Sigma[(\chi_M T)_{obs} - (\chi_M T)_{calcd.}]^2/\Sigma(\chi_M T)_{obs}^2$.

The $\chi_M T$ value of **7** at room temperature is 2.60 $cm^3 mol^{-1} K$ (4.56 μ_B), which is larger than the spin-only value of 1.75 $cm^3 mol^{-1} K$ (3.74 μ_B) per $Ni^{II}Fe^{III}_2$ unit. In a manner similar to those of **1**–**3**, the $\chi_M T$ vs. T plot clearly shows that the Ni^{II} ion and the low-spin Fe^{III} ions are ferromagnetically coupled (Figure 7). The plot of $1/\chi_M$ vs. T in the temperature range 50–300 K obeys the Curie–Weiss law with a positive Weiss constant of 18.91(2) K, which confirms the ferromagnetic interactions between Ni^{II} and Fe^{III}. We tried to use a 1D heteronuclear chain model in the analysis of the magnetic data of Figure 7 by coupling two original S_{Fe} into $S_{Fe'}$ (Scheme 3).[13] However, $S_{Fe'} = S_{Ni} = 1$, which means it is impossible to identify the two

different types of atoms in the 1D heteronuclear chain. Therefore, we used the 1D homonuclear chain model to analyze the magnetic data through the Hamiltonian:[27c]

$$\hat{H} = -2J\sum_i S_{Ni,i}(S_{Fe,i+1,up} + S_{Fe,i+1,down}) = -2J\sum_i S_{Ni,i}S'_{Fe,i+1}$$

$$S'_{Fe,i+1} = S_{Fe,i+1,up} + S_{Fe,i+1,down} \quad \chi = \frac{2N\beta^2g^2S(S+1)}{3kT}\frac{1+u}{1-u}$$

where $u = \coth(x) - 1/x$ and $x = JS(S+1)/kT$. The least-squares fit of the magnetic susceptibility data of **7** gives the fitted values of $J = 12.5(2)\ cm^{-1}$, $g = 2.18(1)$ and $R = 7.8 \times 10^{-4}$.

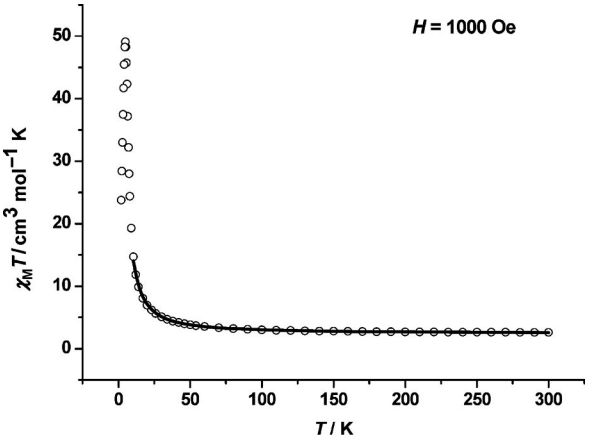

Figure 7. $\chi_M T$ vs. T plot of **7** under an applied field of 1000 Oe in the temperature range 2–300 K: (○) experimental data; (solid line) best-fit curve.

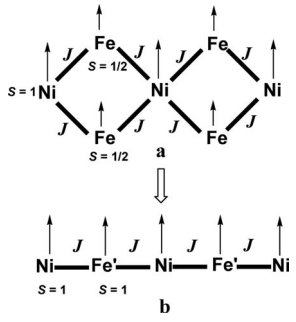

Scheme 3. The analysis process from heteronulcear chain to homonuclear chain.

A metamagnetic behavior is observed from the temperature dependence of the dc magnetization measurements (Figure 8a). At lower dc fields, the M vs. T plots display peaks at 4.8 K (50 and 150 Oe) and 4.4 K (300 Oe), which disappear at a higher dc field (500–2000 Oe). The metamagnetic behavior is also confirmed by the field dependence of the magnetization measurement at 2.0 K (Figure 8b and inset of Figure 8b). The magnetization curve displays an explicit sigmoidal shape, with a critical field $H_c = 359$ Oe from the peak position of the dM/dH vs. H curve. The saturation magnetization value of 4.35 μ_B at 70 kOe is close to the expected value of 4 μ_B for a Fe_2Ni unit, which indicates a ferromagnetic correlation between the adjacent Ni^{II} and Fe^{III} ions in a large applied field. The magnetic properties of **7** can be rationalized on the basis of its structure. As shown in Scheme 4, the ferromagnetic couplings between the Fe^{III} and Ni^{II} ions through the cyanido-bridges within the chain lead to a ferromagnetic chain. At lower fields, the AF interactions between the adjacent chains result in an AF ground state, while a ferromagnetic interaction occurs at higher fields.

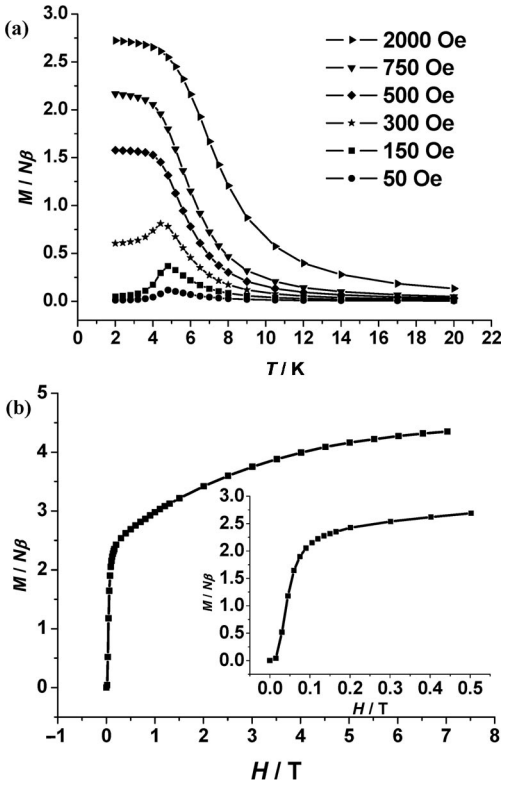

Figure 8. (a) M vs. T plots of **7** under various applied fields. (b) Field dependence of the magnetization of **7** at 2.0 K.

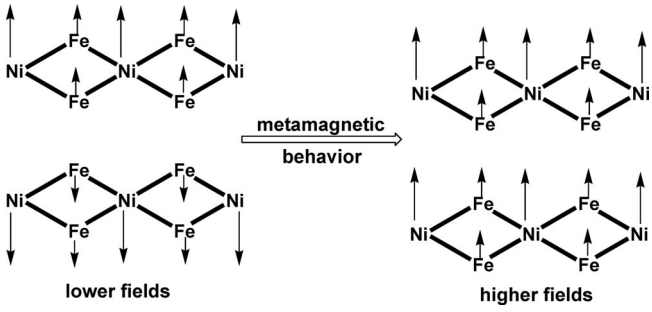

Scheme 4.

The in-phase (χ') and out-of-phase (χ'') components of the ac magnetic susceptibility of **7** were measured under a zero applied dc field and a 5 G oscillating ac field below 10 K (Figure 9). The χ' vs. T plots show a frequency-independent peak at 4.8 K, while the χ'' vs. T plots are nearly linear from 10 K to 3 K. Below 3 K, the χ'' components

are frequency dependent, which is indicative of the presence of slow relaxation of the magnetization as observed for SCMs.[9] A maximum at 2.28 K of the curve at 997 Hz is observed, while the maxima of the other curves at 100 Hz, 10 Hz, and 1 Hz could not be observed because of the limited test temperature range of our SQUID, which precludes the evaluation of the energy barrier.

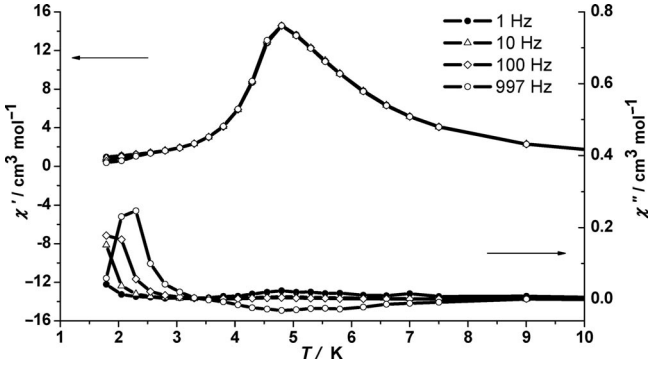

Figure 9. The in-phase (χ') and out-of-phase (χ'') components of the ac magnetic susceptibility under a 5 G oscillating ac field and a zero applied dc field in **7**.

The magnetic behavior of **7** is very different to that of **9**.[26] Firstly, the $\chi_M T$ maximum value (49 $cm^3 mol^{-1} K$) of **7** is much smaller than that of **9** (178 $cm^3 mol^{-1} K$) because of the more bent Ni–N≡C angles in **7**. Secondly, supramolecular isomer **7** shows a metamagnetic behavior, while **9** displays ferromagnetic ordering. Thirdly, the χ'' components of **7** are frequency dependent at low temperature, while **9** shows frequency-independent ac signals. Obviously, the different magnetic behaviors of **7** and **9** originate from the structural difference between these two supramolecular isomers.

Conclusions

In summary, a series of cyanido-bridged dimetallic complexes **1**–**8** was synthesized from the two cyanido precursors $H[Fe(phen)(CN)_4]\cdot 2H_2O$ and $H[Fe(bipy)(CN)_4]\cdot 2H_2O$. Different structural motifs were obtained, from discrete clusters for **1**–**5** to a 2D network for **8**. As expected, ferromagnetic couplings were found in **1**–**3** and **7** between the low-spin Fe^{III} ions (t_{2g}^5) and the Ni^{II} ions (e_g^2) bridged by cyanido groups because of the strict orthogonality of the two magnetic orbitals. A metamagnetic behavior and a frequency-dependent relaxation of χ'' were observed in **7**.

Experimental Section

General Remarks: The cyanido precursors $H[Fe(phen)(CN)_4]\cdot 2H_2O$ and $H[Fe(bipy)(CN)_4]\cdot 2H_2O$ and the macrocyclic complexes $[NiL^1](ClO_4)_2$, $[NiL^2](ClO_4)_2$ and $[CuL^3](ClO_4)_2$ were prepared according to literature methods.[28,29] All of the other reagents of analytical grade were commercially available and used without further purification. Elemental analyses were determined by using Elementar Vario E-L elemental analyser. The IR spectra were recorded in the 400–4000 cm^{-1} region by using KBr pellets and a Bruker EQUINOX 55 spectrometer. Magnetic susceptibility measurements of **1**–**3** and **7** were performed on polycrystalline samples fixed with GE7031 varnish on a Quantum Design MPMS-XL7 SQUID in the temperature range 2–300 K and under an applied field of 1000 G.

$\{[Fe^{III}(phen)(CN)_4]_2[NiL^1]\}\cdot 4H_2O$ (1): An aqueous solution (5 mL) of $H[Fe(phen)(CN)_4]\cdot 2H_2O$ (76 mg, 0.2 mmol) was layered with an acetonitrile solution (5 mL) of $[NiL^1](ClO_4)_2$ (54 mg, 0.1 mmol) in the dark. Dark-red prism-shaped crystals of **1** were isolated after about two weeks. The crystals were collected and washed with a small amount of acetonitrile/water (1:1) and dried in air. Yield: 58% (64 mg, 0.058 mmol). $C_{48}H_{60}Fe_2N_{16}NiO_4$ (1095.53): calcd. C 52.63, H 5.52, N 20.46; found C 52.88, H 5.35, N 20.76. IR (KBr): $\tilde{\nu}_{C\equiv N}$ = 2119 (m), 2135 (m) cm^{-1}.

$\{[Fe^{III}(bipy)(CN)_4]_2[NiL^1]\}\cdot 4H_2O$ (2): This compound was prepared by a similar procedure to that of **1** from $H[Fe(bipy)(CN)_4]\cdot 2H_2O$ (71 mg, 0.2 mmol) and $[NiL^1](ClO_4)_2$ (54 mg, 0.1 mmol). Yield: 51% (53 mg, 0.051 mmol). $C_{44}H_{60}Fe_2N_{16}NiO_4$ (1047.49): calcd. C 50.45, H 5.77, N 21.40; found C 49.83, H 5.55, N 22.05. IR (KBr): $\tilde{\nu}_{C\equiv N}$ = 2141 (m), 2118 (m) cm^{-1}.

$[Fe^{III}(bipy)(CN)_4]_2[NiL^2]$ (3): This compound was prepared by a similar procedure to that of **1** from $H[Fe(bipy)(CN)_4]\cdot 2H_2O$ (71 mg, 0.2 mmol) and $[NiL^2](ClO_4)_2$ (67 mg, 0.1 mmol). Yield: 50% (54 mg, 0.050 mmol). $C_{48}H_{60}Fe_2N_{16}NiO_4$ (1073.49): calcd. C 55.02, H 4.80, N 23.10; found C 54.41, H 4.75, N 23.91. IR (KBr): $\tilde{\nu}_{C\equiv N}$ = 2122 (m), 2139 (m) cm^{-1}.

$\{[Fe^{III}(phen)(CN)_4]_2[CuL^3]\}\cdot 5H_2O$ (4): This compound was prepared by a similar procedure to that of **1** from $H[Fe(phen)(CN)_4]\cdot 2H_2O$ (76 mg, 0.2 mmol) and $[CuL^3](ClO_4)_2$ (55 mg, 0.1 mmol). Yield: 55% (60 mg, 0.055 mmol). $C_{44}H_{51}CuFe_2N_{18}O_7$ (1119.23): calcd. C 47.22, H 4.59, N 22.53; found C 47.53, H 4.92, N 22.18. IR (KBr): $\tilde{\nu}_{C\equiv N}$ = 2121 (m), 2141 (m) cm^{-1}.

$\{[Fe^{II}(phen)(CN)_4][Ni(ea)]\}_2\cdot 2H_2O$ (5): An aqueous solution (5 mL) of $H[Fe(phen)(CN)_4]\cdot 2H_2O$ (76 mg, 0.2 mmol) was layered with a mixture of $Ni(ClO_4)_2\cdot 6H_2O$ (37 mg, 0.1 mmol) and ethanolamine (ea) (12 mg, 0.2 mmol) in acetonitrile (6 mL) in the dark. Violet cubic crystals of **5** were isolated after about two weeks. The crystals were collected, washed with a small amount of acetonitrile/water (1:1), and dried in air. Yield: 61% (68 mg, 0.061 mmol). $C_{40}H_{60}Fe_2N_{16}Ni_2O_8$ (1122.16): calcd. C 42.82, H 5.39, N 19.97; found C 42.13, H 4.80, N 20.24. IR (KBr): $\tilde{\nu}_{C\equiv N}$ = 2067 (m), 2102 (m) cm^{-1}.

$\{[Fe^{II}(phen)(CN)_4][NiL^2]\cdot 2H_2O\}_n$ (6): This compound was prepared by a similar procedure to that of **1** from $H[Fe(phen)(CN)_4]\cdot 2H_2O$ (76 mg, 0.2 mmol) and $[NiL^2](ClO_4)_2$ (67 mg, 0.1 mmol). Yield: 45% (37 mg, 0.045 mmol). $C_{38}H_{45}FeN_{12}NiO_2$ (816.42): calcd. C 55.91, H 5.56, N 20.59; found C 55.86, H 5.52, N 21.38. IR (KBr): $\tilde{\nu}_{C\equiv N}$ = 2064 (m), 2087 (m) cm^{-1}.

$\{[Fe^{III}(bipy)(CN)_4]_2[Ni(H_2O)_2]\cdot 6.5H_2O\}_n$ (7): This compound was prepared by a similar procedure to that of **5**, by replacing ethanolamine with malonic acid (10 mg, 0.1 mmol) and $H[Fe(phen)(CN)_4]\cdot 2H_2O$ with $H[Fe(bipy)(CN)_4]\cdot 2H_2O$ (71 mg, 0.2 mmol). Yield: 40% (34 mg, 0.040 mmol). $C_{28}H_{33}Fe_2N_{12}NiO_{8.5}$ (844.07): calcd. C 39.84, H 3.941, N 19.91; found C 39.22, H 4.305, N 19.83. IR (KBr): $\tilde{\nu}_{C\equiv N}$ = 2122 (m), 2170 (m) cm^{-1}.

$\{[Fe^{II}(bipy)(CN)_4][Ni(ea)_2]\cdot H_2O\}_n$ (8): This compound was prepared by a similar procedure to that of **5**, by replacing $H[Fe(phen)(CN)_4]\cdot 2H_2O$ with $H[Fe(bipy)(CN)_4]\cdot 2H_2O$ (71 mg, 0.2 mmol). Yield: 55% (28 mg, 0.055 mmol). $C_{18}H_{23}FeN_8NiO_3$ (514.00): calcd. C 40.06, H 4.51, N 21.80; found C 40.61, H 4.70, N 21.52. IR (KBr): $\tilde{\nu}_{C\equiv N}$ = 2070 (m), 2109 (m) cm^{-1}.

X-ray Crystallography: X-ray diffraction experiments for single crystals were performed on a Bruker Smart 1000 CCD diffractometer at 173(2) K by using graphite monochromated Mo-K_α radiation (λ = 0.71073 Å). The empirical absorption corrections were applied by using the SADABS program.[30] The structures were solved with the direct method, which yielded the positions of all non-hydrogen atoms. These were refined first isotropically and then anisotropically. All hydrogen atoms of the ligands were placed in calculated positions with fixed isotropic thermal parameters and included in structure factor calculations in the final stage of a full-matrix least-squares refinement. All calculations were performed with the SHELXTL-97 system of computer programs.[31] For **1**, **2**, and **4**, the macrocyclic ligands L^1 and L^3 are disordered. For **2**, **4**, **5**, and **7**, the water molecules are disordered. The crystallographic data for **1**–**8** are listed in Table 1, and the selected bond lengths and angles for **1**–**8** are shown in Table S1. CCDC-705632 (**1**), -705633 (**2**), -705634 (**3**), -705635 (**4**), -705636 (**5**), -705637 (**6**), -705638 (**7**), and -705639 (**8**) contain the supplementary crystallographic data for this paper. These data can be obtained free of charge from the Cambridge Crystallographic Data Centre via www.ccdc.cam.ac.uk/data_request/cif.

Supporting Information (see footnote on the first page of this article): Selected angles and bond lengths for **1**–**8**, hydrogen-bonding distances in **1**, **2**, **4**, and **5**, the structures of **2**–**4**, intermolecular hydrogen-bonding and π···π interactions in **2**, edge-to-face C–H···π interactions in **3**, intermolecular hydrogen-bonding interactions in **4** and **5**, a fragment of the 1D 4,2-ribbonlike chain in **7**, the X shape of the chain along the *c* axis in **7**, the reported 4,2-ribbonlike chain of $\{[Fe^{III}(bipy)(CN)_4]_2[Ni(H_2O)_2]\}\cdot 4H_2O$, and ac signals of **1**–**3** are presented.

Acknowledgments

This work was supported by the Natural Science Foundation of China (20625103, 20831005) and the 973 Program of China (2007CB815305). The authors wish to thank Dr. Yanzhen Zheng at the University of Karlsruhe and Mr. Weixiong Zhang at Sun Yat-Sen University for their assistance in the fitting of the magnetic data.

[1] a) M. Verdaguer, A. Bleuzen, V. Marvaud, J. Vaissermann, M. Seuleiman, C. Desplanches, A. Scuiller, C. Train, R. Garde, G. Gelly, C. Lomenech, I. Rosenman, P. Veillet, C. Cartier, F. Villain, *Coord. Chem. Rev.* **1999**, *190–192*, 1023–1047; b) M. Ohba, H. Okawa, *Coord. Chem. Rev.* **2000**, *198*, 313–328; c) J. Cernák, M. Orendác, I. Potocnák, J. Chomic, A. Horendacová, J. Skorsepa, A. Feher, *Coord. Chem. Rev.* **2002**, *224*, 51–66; d) R. Lescouëzec, L. M. Toma, J. Vaissermann, M. Verdaguer, F. S. Delgado, C. Ruiz-Pérez, F. Lloret, M. Julve, *Coord. Chem. Rev.* **2005**, *249*, 2691–2729.

[2] a) S. S. Kaye, J. R. Long, *J. Am. Chem. Soc.* **2005**, *127*, 6506–6507; b) S. S. Kaye, J. R. Long, *Chem. Commun.* **2007**, 4486–4488.

[3] a) R. Brahmi, C. Kappenstein, J. Cernák, D. Duprez, A. Sadel, *J. Chim. Phys. Phys.-Chim. Biol.* **1999**, *96*, 487–497; b) D. J. Darensbourg, A. L. Phelps, *Inorg. Chim. Acta* **2004**, *357*, 1603–1607.

[4] a) D. Williams, J. Kouvetakis, M. O'Keefe, *Inorg. Chem.* **1998**, *37*, 4617–4620; b) M. P. Shores, L. G. Beauvais, J. R. Long, *J. Am. Chem. Soc.* **1999**, *121*, 775–779; c) M. P. Shores, L. G. Beauvais, J. R. Long, *Inorg. Chem.* **1999**, *38*, 1648–1649; d) M. P. Bennett, L. G. Beauvais, M. P. Shores, J. R. Long, *J. Am. Chem. Soc.* **2001**, *123*, 8022–8032.

[5] a) T. Mallah, S. Thiébault, M. Verdaguer, P. Veillet, *Science* **1993**, *262*, 1554–1557; b) S. Ferlay, T. Mallah, R. Ouhaès, P. Veillet, M. Verdaguer, *Nature* **1995**, *378*, 701–703; c) W. R. Entley, G. S. Girolami, *Science* **1995**, *268*, 397–400; d) Ø. Hatlevik, W. E. Buschmann, J. Zhang, J. L. Manson, J. S. Miller, *Adv. Mater.* **1999**, *11*, 914–918; e) S. M. Holmes, G. S. Girolami, *J. Am. Chem. Soc.* **1999**, *121*, 5593–5594; f) R. Garde, F. Villain, M. Verdaguer, *J. Am. Chem. Soc.* **2002**, *124*, 10531–10538.

[6] a) O. Sato, T. Iyoda, A. Fujishima, K. Hashimoto, *Science* **1996**, *271*, 49–51; b) O. Sato, S. Hayami, Y. Einaga, Z.-Z. Gu, *Bull. Chem. Soc. Jpn.* **2003**, *76*, 443–470.

[7] a) K. Inoue, K. Kikuchi, M. Ohba, H. Okawa, *Angew. Chem. Int. Ed.* **2003**, *42*, 4810–4813; b) W. Kaneko, S. Kitagawa, M. Ohba, *J. Am. Chem. Soc.* **2007**, *129*, 248–249; c) O. Sereda, J. Ribas, H. Stoeckli-Evans, *Inorg. Chem.* **2008**, *47*, 5107–5113.

[8] a) J. J. Sokol, A. G. Hee, J. R. Long, *J. Am. Chem. Soc.* **2002**, *124*, 7656–7657; b) C. P. Berlinguette, D. Vaughn, C. Canada-Vilalta, J. R. Galán-Mascaroś, K. R. Dunbar, *Angew. Chem. Int. Ed.* **2003**, *42*, 1523–1526; c) V. S. Mironov, L. F. Chibotaru, A. Ceulemans, *J. Am. Chem. Soc.* **2003**, *125*, 9750–9760; d) H. J. Choi, J. J. Sokol, J. R. Long, *Inorg. Chem.* **2004**, *43*, 1606–1608; e) E. J. Schelter, A. V. Prosvirin, K. R. Dunbar, *J. Am. Chem. Soc.* **2004**, *126*, 15004–15005; f) E. J. Schelter, F. Karadas, C. Avendano, A. V. Prosvirin, W. Wernsdorfer, K. R. Dunbar, *J. Am. Chem. Soc.* **2007**, *129*, 8139–8149.

[9] a) R. Lescouëzec, J. Vaissermann, C. Ruiz-Pérez, F. Lloret, R. Carrasco, M. Julve, M. Verdaguer, Y. Dromzee, D. Gatteschi, W. Wernsdorfer, *Angew. Chem. Int. Ed.* **2003**, *42*, 1483–1486; b) L. M. Toma, R. Lescouëzec, F. Lloret, M. Julve, J. Vaissermann, M. Verdaguer, *Chem. Commun.* **2003**, 1850–1851; c) S. Wang, J. L. Zuo, S. Gao, Y. Song, H. C. Zhou, Y. Z. Zhang, X. Z. You, *J. Am. Chem. Soc.* **2004**, *126*, 8900–8901.

[10] a) J. H. Yoon, H. C. Kim, C. S. Hong, *Inorg. Chem.* **2005**, *44*, 7714–7716; b) S. Wang, M. Ferbinteanu, M. Yamashita, *Inorg. Chem.* **2007**, *46*, 610–612; c) J. H. Yoon, J. H. Lim, S. W. Choi, H. C. Kim, C. S. Hong, *Inorg. Chem.* **2007**, *46*, 1529–1531; d) J. I. Kim, H. S. Yoo, E. K. Koh, C. S. Hong, *Inorg. Chem.* **2007**, *46*, 10461–10463.

[11] a) S. Bonhommeau, G. Molnar, A. Galet, A. Zwick, J.-A. Real, J. J. McGarvey, A. Bousseksou, *Angew. Chem. Int. Ed.* **2005**, *44*, 4069–4073; b) M. Nihei, M. Ui, M. Yokota, L. Han, A. Maeda, H. Kishida, H. Okamoto, H. Oshio, *Angew. Chem. Int. Ed.* **2005**, *44*, 6484–6487; c) S. Cobo, G. Molnar, J. A. Real, A. Bousseksou, *Angew. Chem. Int. Ed.* **2006**, *45*, 5786–5789; d) M. Shatruk, A. Dragulescu-Andrasi, K. E. Chambers, S. A. Stoian, E. L. Bominaar, C. Achim, K. R. Dunbar, *J. Am. Chem. Soc.* **2007**, *129*, 6104–6116; e) F. Volatron, L. Catala, E. Riviere, A. Gloter, O. Stephan, T. Mallah, *Inorg. Chem.* **2008**, *47*, 6584–6586.

[12] a) C. P. Berlinguette, A. Dragulescu-Andrasi, A. Sieber, J. R. Galan-Mascaros, H.-U. Guedel, C. Achim, K. R. Dunbar, *J. Am. Chem. Soc.* **2004**, *126*, 6222–6223; b) C. P. Berlinguette, A. Dragulescu-Andrasi, A. Sieber, H.-U. Guedel, C. Achim, K. R. Dunbar, *J. Am. Chem. Soc.* **2005**, *127*, 6766–6779; c) M. Nihei, M. Ui, N. Hoshino, H. Oshio, *Inorg. Chem.* **2008**, *47*, 6106–6108.

[13] Y.-Z. Zhang, S. Gao, Z.-M. Wang, G. Su, H.-L. Sun, F. Pan, *Inorg. Chem.* **2005**, *44*, 4534–4545.

[14] Y.-Z. Zhang, Z.-M. Wang, S. Gao, *Inorg. Chem.* **2006**, *45*, 10404–10406.

[15] L. Toma, R. Lescouëzec, J. Vaissermann, F. S. Delgado, C. Ruiz-Pérez, R. Carrasco, J. Cano, F. Lloret, M. Julve, *Chem. Eur. J.* **2004**, *10*, 6130–6145.

[16] R. Lescouëzec, F. Lloret, M. Julve, J. Vaissermann, M. Verdaguer, *Inorg. Chem.* **2002**, *41*, 818–826.

[17] L. Toma, L. M. Toma, R. Lescouëzec, D. Armentano, G. D. Munno, M. Andruh, J. Cano, F. Lloret, M. Julve, *Dalton Trans.* **2005**, 1357–1364.

[18] L. M. Toma, R. Lescouëzec, L. D. Toma, F. Lloret, M. Julve, J. Vaissermann, M. Andruh, *J. Chem. Soc., Dalton Trans.* **2002**, 3171–3176.

[19] Y.-Z. Zhang, S. Gao, H.-L. Sun, G. Su, Z.-M. Wang, F. Pan, S.-W. Zhang, *Chem. Commun.* **2004**, 1906–1907.
[20] L. Toma, R. Lescouëzec, J. Vaissermann, P. Herson, V. Marvaud, F. Lloret, M. Julve, *New J. Chem.* **2005**, *29*, 210–219.
[21] L. M. Toma, F. S. Delgado, C. Ruiz-Pérez, R. Carrasco, J. Cano, F. Lloret, M. Julve, *Dalton Trans.* **2004**, 2836–2846.
[22] R. Lescouëzec, F. Lloret, M. Julve, J. Vaissermann, M. Verdaguer, R. Llusar, S. Uriel, *Inorg. Chem.* **2001**, *40*, 2065–2072.
[23] F. Pan, Z.-M. Wang, S. Gao, *Inorg. Chem.* **2007**, *46*, 10221–10228.
[24] Y.-Z. Zhang, Z.-M. Wang, S. Gao, *Inorg. Chem.* **2006**, *45*, 5447–5454.
[25] L. Jiang, X.-L. Feng, T.-B. Lu, S. Gao, *Inorg. Chem.* **2006**, *45*, 5018–5026.
[26] L. M. Toma, R. Lescouëzec, S. Uriel, R. Llusar, C. Ruiz-Pérez, J. Vaissermann, F. Lloret, M. Julve, *Dalton Trans.* **2007**, 3690–3698.
[27] a) O. Kahn in *Molecular Magnetism*, VCH Publishers, New York, **1993**, p. 211–213; b) Y.-H. Zhang, M. Yu, Q.-L. Wang, G.-F. Xu, M. Hu, G.-M. Yang, D.-Z. Liao, *Polyhedron* **2008**, *27*, 3371–3376; c) O. Kahn in *Molecular Magnetism*, VCH Publishers, New York, **1993**, p. 257–259.
[28] A. A. Schildt, *J. Am. Chem. Soc.* **1960**, *82*, 3000–3005.
[29] a) M. P. Suh, B. Y. Shim, T. S. Yoon, *Inorg. Chem.* **1994**, *33*, 5509–5514; b) T.-B. Lu, H. Xiang, X.-Y. Li, Z.-W. Mao, L.-N. Ji, *Inorg. Chem. Commun.* **2000**, *3*, 597–599.
[30] G. M. Sheldrick, *SADABS, Program for Empirical Absorption Correction of Area Detector Data*, University of Göttingen, Göttingen, Germany, **1996**.
[31] G. M. Sheldrick, *SHELXTL-97, Program for Crystal Structure Solution and Refinement*, University of Göttingen, Göttingen, Germany, **1997**.

Received: February 7, 2009
Published Online: March 27, 2009

